



## Opinion percolation in structured population



Han-Xin Yang<sup>a,\*</sup>, Liang Huang<sup>b</sup>

<sup>a</sup> Department of Physics, Fuzhou University, Fuzhou 350108, China

<sup>b</sup> Institute of Computational Physics and Complex Systems, Lanzhou University, Lanzhou, Gansu 730000, China

### ARTICLE INFO

#### Article history:

Received 23 January 2014

Received in revised form

4 March 2015

Accepted 6 March 2015

Available online 18 March 2015

#### Keywords:

Complex networks

Opinion

Percolation

### ABSTRACT

In a recent work (Shao et al., 2009), a nonconsensus opinion (NCO) model was proposed, where two opinions can stably coexist by forming clusters of agents holding the same opinion. The NCO model on lattices and several complex networks displays a phase transition behavior, which is characterized by a large spanning cluster of nodes holding the same opinion appears when the initial fraction of nodes holding this opinion is above a certain critical value. In the NCO model, each agent will convert to its opposite opinion if there are more than half of agents holding the opposite opinion in its neighborhood. In this paper, we generalize the NCO model by assuming that each agent will change its opinion if the fraction of agents holding the opposite opinion in its neighborhood exceeds a threshold  $T$  ( $T \geq 0.5$ ). We call this generalized model as the NCOT model. We apply the NCOT model on different network structures and study the formation of opinion clusters. We find that the NCOT model on lattices displays a continuous phase transition. For random graphs and scale-free networks, the NCOT model shows a discontinuous phase transition when the threshold is small and the average degree of the network is large, while in other cases the NCOT model displays a continuous phase transition.

© 2015 Elsevier B.V. All rights reserved.

### 1. Introduction

The dynamics of opinion sharing and competing has become an active topic of recent research in statistical physics [1]. One of the most successful methodologies used in opinion dynamics is agent-based modeling [1]. The idea is to construct the computational devices (known as agents with some properties) and then simulate them in parallel to model the real phenomena. In physics this technique can be traced back to Monte Carlo (MC) simulations [2]. Beyond relevance as physics models, the ferromagnetic Ising model [3–5], the XY model [6] and the Potts model [7,8] can be seen as agent-based models for opinion dynamics. Other versions of opinion models have also been proposed, such as the Sznajd model [9], the majority rule model [10–12], the voter model [13,14], and the social impact model [15]. Some models display a disorder–order transition [16–25], from a regime in which opinions are arbitrarily diverse to one in which most individuals hold the same opinion. Other models focus the emergence of a global consensus, in which all agents finally share the same opinion [26–36].

\* Corresponding author.

E-mail addresses: [hxyang01@gmail.com](mailto:hxyang01@gmail.com) (H.-X. Yang), [huangl@lzu.edu.cn](mailto:huangl@lzu.edu.cn) (L. Huang).

<http://dx.doi.org/10.1016/j.cpc.2015.03.004>

0010-4655/© 2015 Elsevier B.V. All rights reserved.

It has been known that the formation of opinion clusters plays an important role in opinion dynamics [37,27,38,39]. An opinion cluster is defined as a connected component (subgraph) fully occupied by nodes holding the same opinion. Recently, Shao et al. proposed a nonconsensus opinion (NCO) model [40] in which each node adopts the majority opinion in its neighborhood at each time step. It was found that a large spanning cluster of nodes holding the same opinion appears when the initial fraction of nodes holding this opinion exceeds a certain threshold [40,41]. Motivated by the NCO model, Li et al. proposed an inflexible contrarian opinion (ICO) model in which some agents never change their original opinion but may influence the opinions of others [42]. It was found that the threshold above which a large spanning cluster appears is increased with the fraction of inflexible contrarians.

In both the NCO and ICO models, an agent will adopt the opinion that is held by more than half of neighbors. However, in many real-life situations, a quorum far larger than one half is necessary to pass a resolution. For example, a referendum to recall the president of the United States requires the support of two-thirds of the senators. Based on the above reasons, in this paper we generalize the NCO model by assuming that an agent will change its opinion when the fraction of agents holding the opposite opinion in its neighborhood exceeds a threshold  $T \geq 0.5$ . We call this generalized model as the NCOT model. When the threshold  $T = 0.5$ , the NCOT model recovers to the NCO model. When  $T = 1$ , the NCOT model becomes

the standard percolation without opinion dynamics. Both the NCO and ICO models focus on the critical value for finite-size networks. By the standard finite-size scaling approach, we have obtained a critical point at which the phase transition takes place in the limit of infinite network size. It is interesting to find that, continuous or discontinuous phase transitions can arise in the NCOT model, depending on the value of  $T$  and the network structure.

The paper is organized as follows. In Section 2, we introduce the NCOT model. In Section 3, we study the NCOT model on square lattices, random networks and scale-free networks, respectively. Finally, conclusions and discussions are presented in Section 4.

## 2. A nonconsensus opinion model with the threshold (NCOT)

In the NCOT model on networks, each node holds one of the binary opinions denoted by  $+1$  and  $-1$ . Initially, a fraction  $f$  of nodes with the opinion  $+1$  and  $1 - f$  with the opinion  $-1$  are selected at random. The neighborhood of node  $i$  is composed of node  $i$  and its nearest neighbors. At each time step, each node will convert to its opposite opinion, if the fraction of nodes holding the opposite opinion in its neighborhood exceeds a threshold  $T$  ( $T \geq 0.5$ ). The system is considered to reach a stable state if no more changes occur.

## 3. Main results

We focus on the formation of opinion clusters in the NCOT model. We denote by  $S_1$  the size of the largest  $+1$  cluster and  $S_2$  the size of the second largest  $+1$  cluster in the steady state. Then we define  $s_1 = S_1/N$  and  $s_2 = S_2/N$ , where  $N$  is the network size. In the following, we carry out simulations systematically by employing the NCOT model on square lattices, random networks and scale-free networks respectively.

### 3.1. The NCOT model on square lattices

In this subsection, we study the NCOT model on an  $N = L \times L$  square lattice with periodic boundary conditions. Our extensive numerical simulations reveal that the phase transition of the NCOT model on square lattice can be roughly divided into three regimes (different universality classes of percolation) by tuning the parameter  $T$ , namely,  $T \in [0.5, 0.6)$ ,  $[0.6, 0.8)$  and  $[0.8, 1]$ . In the same regime, the results are insensitive to the values of  $T$ . Particularly, it is noted that for  $0.5 \leq T < 0.6$ , the corresponding phase transition pertains to the class of invasion percolation with trapping [40]; while for  $0.8 \leq T \leq 1$ , it gives rise to a phase transition subjecting to regular site percolation. The percolation threshold is  $f_c \simeq 0.506$  for  $T \in [0.5, 0.6)$  [40] and  $f_c \simeq 0.5927$  for  $T \in [0.8, 1]$  [43], respectively. For  $0.6 \leq T < 0.8$ , the phase transition has some interesting features and has not been reported before, which will be a focus for this section. To be specific, in the following simulation, we choose  $T = 0.7$ .

Fig. 1 shows the normalized size of the largest cluster  $s_1$  and the second largest cluster  $s_2$  as a function of  $f$  when  $T = 0.7$  and  $N = 10^6$ . We find that there exists a critical value  $f_c(N)$ , below which  $s_1$  approaches 0 and above which  $s_1$  continuously increases as  $f$  increases. At the critical value  $f_c(N)$ ,  $s_2$  displays a sharp peak, a characteristic of a second-order phase transition [40]. Fig. 2 shows the normalized size of the second largest cluster  $s_2$  as a function of  $f$  for different values of  $N$ . From Fig. 2, we observe that the location of  $f_c(N)$  changes with  $N$ . The percolation threshold  $f_c(N)$  of a system of finite size  $N$  obeys the relation [44]

$$f_c(N) - f_c \sim N^{-1/\nu}, \quad (1)$$

where  $f_c$  is the percolation threshold for a system of infinite size and  $\nu$  is the correlation critical exponent. Then a simple linear fit

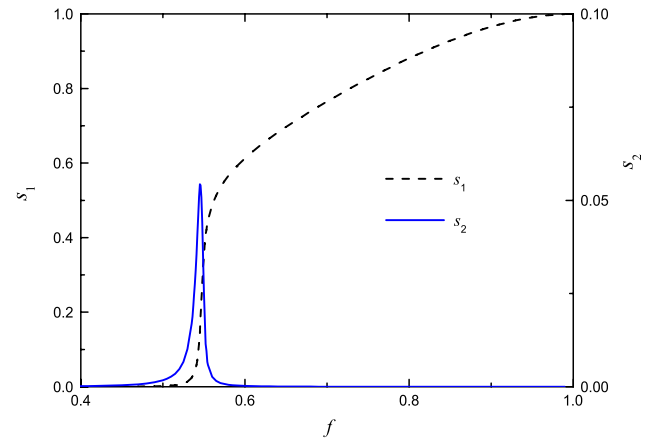


Fig. 1. The normalized size of the largest cluster  $s_1$  and the second largest cluster  $s_2$  as a function of  $f$  on a  $1000 \times 1000$  square lattice.  $T = 0.7$ . Each curve is an average of 1000 different realizations.

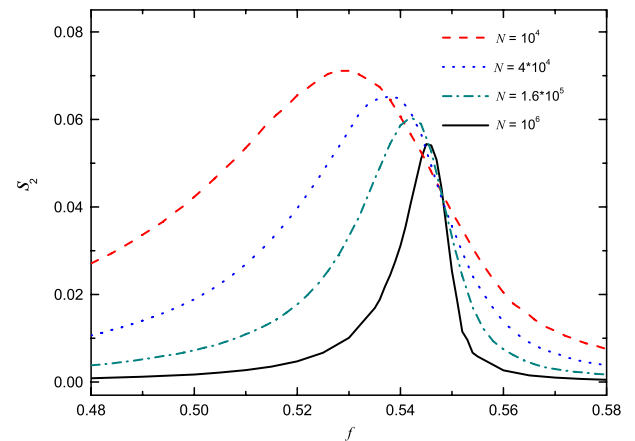


Fig. 2. The normalized size of the second largest cluster  $s_2$  as a function of  $f$  on a square lattice with different values of  $L$ .  $T = 0.7$ . Each curve is an average of 10000, 5000, 3000 and 1000 realizations for  $L = 100, 200, 400$  and  $1000$ , respectively.

(based on the maximization of Pearson's correlation coefficient) of  $f_c(N)$  versus  $N^{-1/\nu}$  allows to simultaneously compute both values of  $f_c$  and  $\nu$  [45,46]. At the percolation threshold  $f_c$ , the normalized size of the largest cluster  $s_1$  and the susceptibility  $\chi = N\sqrt{\langle s_1^2 \rangle - \langle s_1 \rangle^2}$  versus the system size  $N$  follow a power-law form:  $s_1 \sim N^{-\beta/\nu}$  and  $\chi \sim N^{\gamma/\nu}$ .

From simulation results, we obtain  $f_c \simeq 0.5492$  for  $T = 0.7$ . Fig. 3 shows  $f_c - f_c(N)$ ,  $s_1$  and  $\chi$  as a function of  $N$  respectively. From Fig. 3(a)–(c), we estimate the critical exponents  $1/\nu = 0.36(1)$ ,  $\beta/\nu = 0.054(1)$  and  $\gamma/\nu = 0.955(8)$  as the best fit of the data points.

For square lattice, our numerical simulations reveal that the critical point  $f_c$  increases as  $T$  becomes larger. This is because for square lattice, the critical point  $f_c$  is typically larger than 0.5. Thus in this region, a larger  $T$  hinders the transition of opinion  $-1$  to  $+1$  as it requires more  $+1$  neighbors, reducing the final fraction of  $+1$  nodes in the steady state, which in turn, will need a larger  $f$  for the spanning cluster of opinion  $+1$  to emerge.

### 3.2. The NCOT model on random networks

In this subsection, we study the NCOT model on Erdős–Rényi (ER) random networks [47]. ER networks are characterized by a Poisson degree distribution with  $P(k) = e^{-\langle k \rangle} \langle k \rangle^k / k!$ , where  $k$  is the degree of a node and  $\langle k \rangle$  is the average degree of the network.

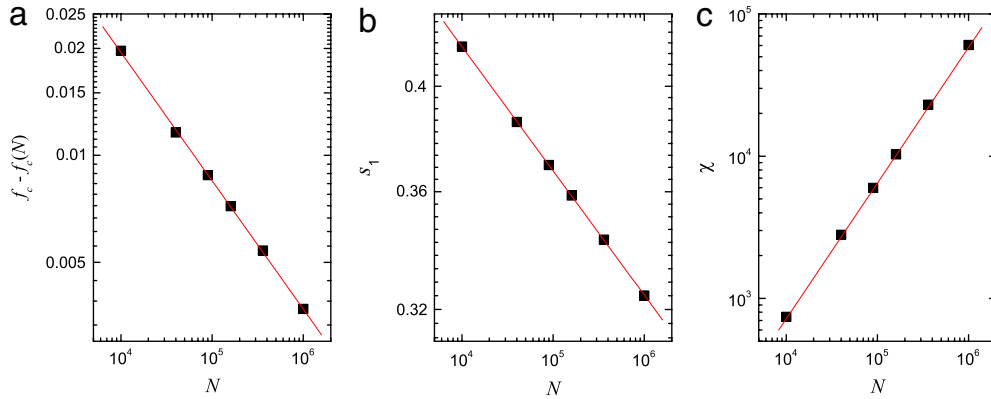


**Fig. 3.** (Color online) Log–log plot of (a)  $f_c - f_c(N)$ , (b) the normalized size of the largest cluster  $s_1$  and (c) the susceptibility  $\chi$ , as a function of the system size  $N$ , respectively. The percolation threshold  $f_c \simeq 0.5492$  for  $T = 0.7$ . In (a)–(c), The slopes of fitted lines are  $-0.36(1)$ ,  $-0.054(1)$  and  $0.955(8)$  respectively. Each data point is an average of 10 000, 5000, 4000, 3000, 2000 and 1000 realizations for  $L = 100, 200, 300, 400, 600$  and  $1000$ , respectively.

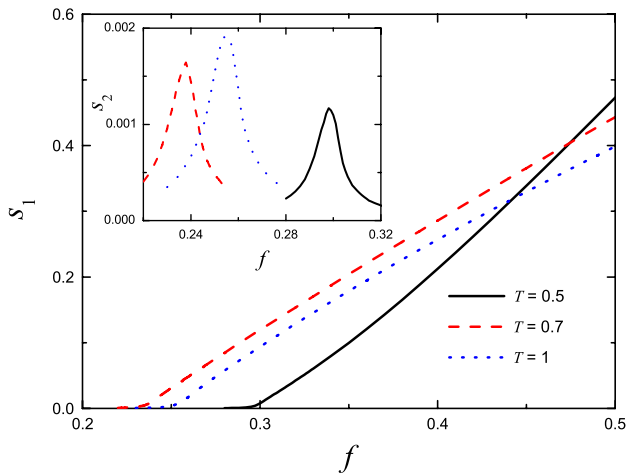


**Fig. 4.** The normalized size of the largest cluster  $s_1$  as a function of  $f$  for different values of  $T$ . The insets shows the normalized size of the second largest cluster  $s_2$  versus  $f$  for different values of  $T$ . The ER network size  $N = 10^6$  and the average degree  $\langle k \rangle = 4$ .

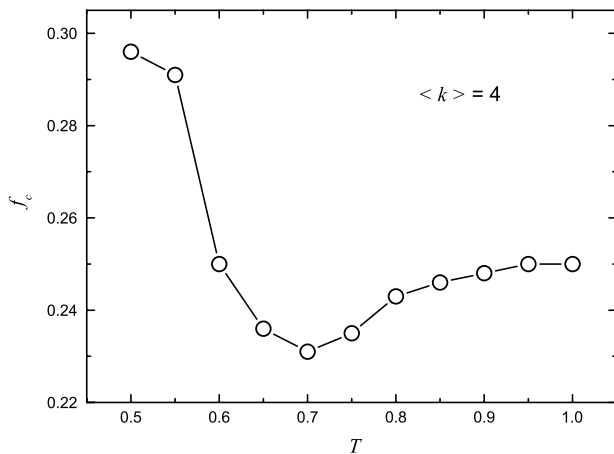


**Fig. 5.** The percolation threshold  $f_c$  as a function of  $T$  on ER networks with the average degree  $\langle k \rangle = 4$ .

We perform simulations with different network sizes  $N$ . Each data point presented below is an average over 10 000, 8000, 6000, 4000, 3000, 2000 and 1000 different realizations for  $N = 10^4, 2 \times 10^4, 5 \times 10^4, 10^5, 2 \times 10^5, 5 \times 10^5$  and  $10^6$ , respectively.

We have found that, when the average degree is small, the phase transition is continuous, while when the average degree is adequately large, depending on  $T$ , the transition can become discontinuous.

To be specific, we have found that when the average degree  $\langle k \rangle = 4$ , the opinion percolation belongs to a continuous phase transition for the whole range of the parameter  $T$ . As shown in Fig. 4, for different values of  $T$  ranging from 0.5 to 1, the normalized size of the largest cluster  $s_1$  continuously increases with  $f$  and the normalized size of the second largest cluster  $s_2$  peaks at a certain critical value of  $f$ . Fig. 5 shows the percolation threshold  $f_c$  as a function of  $T$  when the average degree  $\langle k \rangle = 4$ . The general trend is that as  $T$  increases, the critical threshold  $f_c$  decreases. This can be understood that when  $T = 0.5$ , a node switches its opinion when half of its neighbors (including itself) has the opposite opinion, therefore nodes tend to form clusters with the same opinions. But since  $T$  is small, the cluster is not compact, but rather sparsely connected. In the region where the initial fraction of nodes with  $+1$  opinion  $f < 0.5$ , nodes with  $-1$  are majority, the node is more likely to be surrounded by neighbors with opposite opinions. Thus if  $T$  is small, a node with  $+1$  is more likely to switch to  $-1$ , therefore the effective fraction of nodes with  $+1$  becomes smaller, making it more difficult for a spanning cluster to emerge. As  $T$  increases, it is harder for a node to switch its opinion (requires more neighbors with opposite opinions), leading to a larger effective fraction of nodes with  $+1$ , and therefore a higher probability for a spanning cluster to emerge. Note that the effective fraction of nodes with  $+1$  will still be smaller than  $f$  since nodes with  $-1$  are still majorities therefore more nodes with  $+1$  will be switched to  $-1$  than the opposite process.

A surprising phenomenon is that there exists an optimal value of  $T$  (about 0.7) leading to the minimum of  $f_c$ . This could be a result of higher order interaction between the network topology and the opinion dynamics. For example, although a larger  $T$  means more difficult for a node to switch its opinion, but once the condition is satisfied and this node switches, the cluster grows and it will be more compact, and it will be more resistive to changes caused by outside nodes, leading to a nonmonotonic behavior of  $f_c$  versus  $T$ . The nonmonotonic relation between  $f_c$  and  $T$  can also be confirmed in Fig. 4. From Fig. 4, we can see that the critical value of  $f$  that corresponds to the peak of  $s_2$  is the smallest when  $T = 0.7$ .

When the average degree  $\langle k \rangle$  is adequately large (e.g.,  $\langle k \rangle = 10$ ), the opinion percolation can display a continuous or a discontinuous phase transition, depending on the value of  $T$ . Fig. 6 shows the normalized size of the largest cluster  $s_1$  as a function of  $f$  for different values of  $T$  when  $\langle k \rangle = 10$ . From Fig. 6(a) and (b), we observe that there exist two abrupt transition points when  $T$  is small

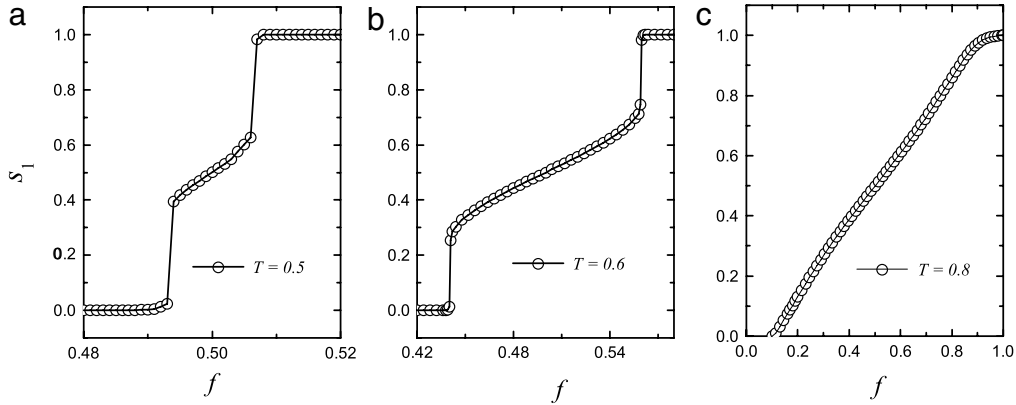


**Fig. 6.** The normalized size of the largest cluster  $s_1$  as a function of  $f$  for (a)  $T = 0.5$ , (b)  $T = 0.6$  and (c)  $T = 0.8$ . The ER network size  $N = 10^6$  and the average degree  $\langle k \rangle = 10$ .

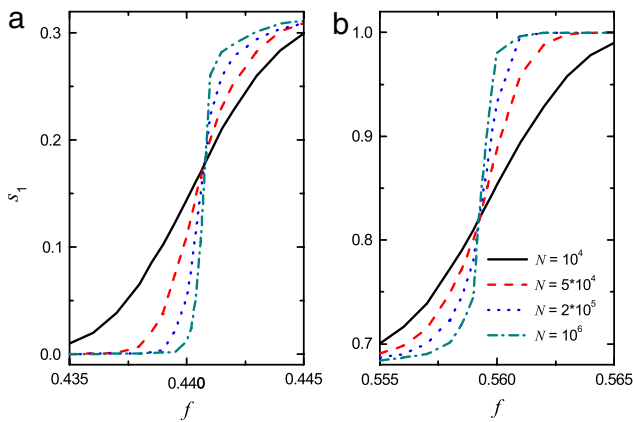


**Fig. 7.** The normalized size of the largest cluster  $s_1$  as a function of  $f$  for different values of the network size  $N$ . The average degree of ER networks is  $\langle k \rangle = 10$  and  $T = 0.6$ . The initial fraction of nodes with the +1 opinion  $f$  is around  $f_c$  for (a) and  $f$  is around  $f_c^*$  for (b).

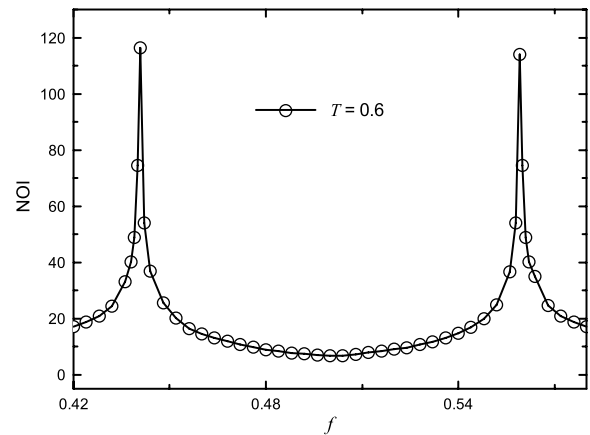


**Fig. 8.** The number of iterations (NOI) as a function of  $f$  on ER networks. The network size  $N = 10^6$ , the average degree  $\langle k \rangle = 10$  and  $T = 0.6$ .

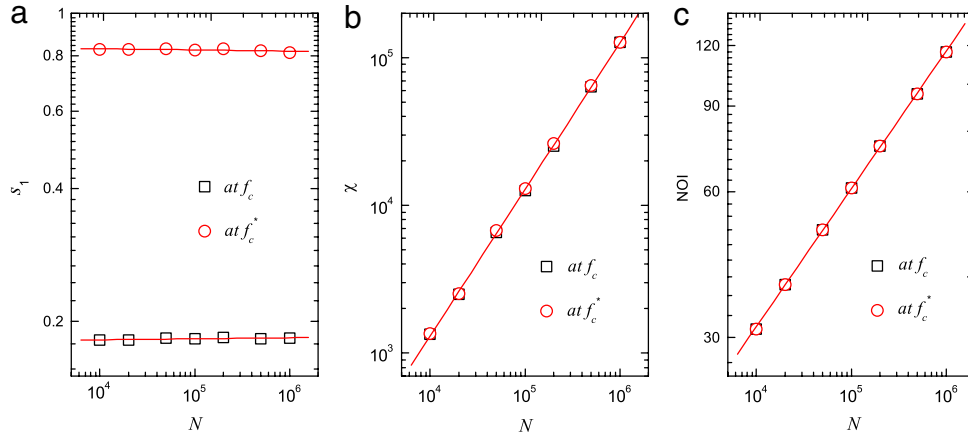
(e.g.,  $T = 0.5$  and  $T = 0.6$ ). At the first abrupt transition point denoted by  $f_c$ ,  $s_1$  jumps from zero to a finite value. At the second abrupt transition point denoted by  $f_c^*$ ,  $s_1$  jumps from a finite value to one. Between the two abrupt transition points,  $s_1$  continuously increases with  $f$ . However, for the large value of  $T$  (e.g.,  $T = 0.8$ ),  $s_1$  approaches zero continuously as  $f$  is decreased from 1 to 0 (see Fig. 6(c)). These numerical results indicate that the behavior of  $s_1$  versus  $f$  could be a discontinuous phase transition for the small value of  $T$  and a continuous phase transition for the large value of  $T$ . From Fig. 6, it is seen that the system has a symmetry, i.e., the curves are unchanged if  $f \rightarrow 1 - f$  and  $s_1 \rightarrow 1 - s_1$ . This is because, in this case, the nodes are densely connected, therefore one can neglect the small clusters for either +1 or -1 opinions. Denote  $s_1^*$  as the normalized size for the largest cluster for -1, we have  $s_1 + s_1^* \approx 1$ . Since the dynamics for the evolution of +1 into -1 and vice versa are the same, this imposes a duality between +1 and -1 states. Therefore, for a given  $f$  after the opinion dynamics reach the steady state the normalized size of the largest cluster for +1 is  $s_1$ , is actually the same process for -1 opinions with a given initial fraction  $1 - f$  and a largest cluster with normalized size  $s_1^*(f) \approx 1 - s_1(f)$ . But since the dynamics for +1 and -1 are the same, when the initial fraction for +1 is  $1 - f$ , the largest cluster for +1 will also be  $s_1^*(f)$ , which is approximately  $1 - s_1(f)$ .

Fig. 7 shows that  $s_1$  as a function of  $f$  for different values of the network size  $N$  when  $\langle k \rangle = 10$  and  $T = 0.6$ . One can see that all the curves intersect at one point (the phase transition point). In Fig. 8, we investigate the number of iterations (NOI), which is the

number of time steps needed to reach the steady state, as a function of  $f$  when  $\langle k \rangle = 10$  and  $T = 0.6$ . Note that NOI characterizes the long range correlation, i.e., if the correlation is local, the system will quickly settle down to the steady state; while if there exist long range correlations, it needs more iterations to reach the steady state since each status change for a node has wider impacts. We can observe that the NOI exhibits two symmetric peaks. According to Ref. [48], in a discontinuous phase transition, the location of the peak of the NOI determines the critical threshold of the transition. In Fig. 8, the location of the left peak determines the critical threshold  $f_c$  below which  $s_1 = 0$  and the right peak determines the critical threshold  $f_c^*$  above which  $s_1 = 1$ . From simulation results shown in Figs. 7 and 8, for  $\langle k \rangle = 10$  and  $T = 0.6$ , we obtain  $f_c \simeq 0.4408$  and  $f_c^* \simeq 0.5592$ . It is noted that  $f_c + f_c^* = 1$ , which is consistent with the previous symmetry analysis.

To further classify the transition class, we carry out finite size scaling analysis. Fig. 9 shows the normalized size of the largest cluster  $s_1$ , the susceptibility  $\chi$  and the number of iterations (NOI), as a function of the system size  $N$  at the discontinuous transition points  $f_c$  and  $f_c^*$ , respectively. Fig. 9(a) shows that  $s_1$  scales as  $N^{-\beta/\nu}$ , with  $\beta/\nu \approx 0$ , indicating a discontinuous phase transition. Fig. 9(b) illustrates that  $\chi$  scales as  $N^{\gamma/\nu}$ , with  $\gamma/\nu \approx 1$ . Fig. 9(c) shows that NOI scales as  $N^\delta$ , with  $\delta \approx 0.28$ , consistent with the theoretical result  $1/4$  [48].

Fig. 10 shows the percolation threshold  $f_c$  as a function of  $T$  when the average degree  $\langle k \rangle = 10$ . One can see that  $f_c$  decreases to 0.1 as  $T$  increases. There exists a certain critical value  $T_c$  (between 0.7 and 0.75), below which the phase transition is discontinuous while above which the phase transition becomes continuous. The



**Fig. 9.** Log-log plot of (a) the normalized size of the largest cluster  $s_1$ , (b) the susceptibility  $\chi$  and (c) the number of iterations (NOI), as a function of the system size  $N$ , respectively. In (a)–(c), The slopes of fitted lines are about 0, 1 and 0.28 respectively. The average degree of ER networks  $\langle k \rangle = 10$  and  $T = 0.6$ . The phase transition points are  $f_c \simeq 0.4408$  and  $f_c^* \simeq 0.5592$ .

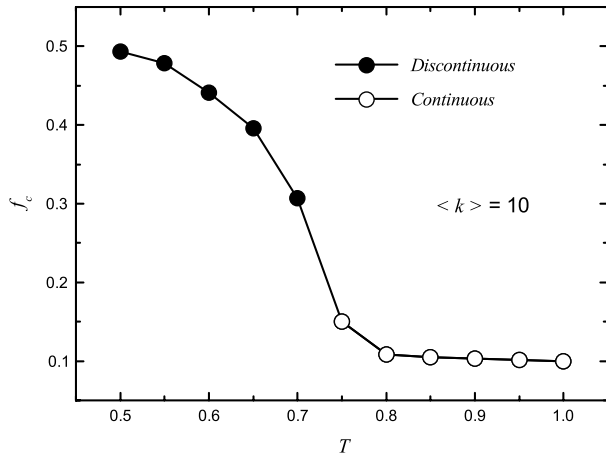


**Fig. 10.** The percolation threshold  $f_c$  as a function of  $T$  on ER networks with the average degree  $\langle k \rangle = 10$ . The phase transition is discontinuous for small values of  $T$  (filled circles), while it becomes continuous for large values of  $T$  (empty circles).

development to the first-order-like phase transition is originated to the consolidation of clusters with the same opinions [49,50]. Two key factors are needed. The first one is the network topology, which needs to be dense enough in order to promote clustering process during the evolution of the opinions [41]. The second one is the opinion dynamics, where  $T$  should be small to lower the barrier for a node to switch its opinion to facilitate the formation of clusters. Therefore, in the region when  $\langle k \rangle$  is large and  $T$  is small, one could expect disrupt emerging of spanning clusters; while in the opposite case when  $\langle k \rangle$  is small and  $T$  is large, one would expect continuous transitions.

### 3.3. The NCOT model on scale-free networks

In this subsection, we study the NCOT model on Barabási–Albert scale-free networks (BA) [51]. BA networks are characterized by a power-law degree distribution with  $P(k) \sim k^{-3}$ . We perform simulations with different network sizes  $N$ . Each data point is an average over 10 000, 6000, 4000, 3000, 2000 and 1000 different realizations for  $N = 10^4, 2 \times 10^4, 5 \times 10^4, 10^5, 2 \times 10^5$  and  $5 \times 10^5$ , respectively.

Fig. 11 shows the normalized size of the largest cluster  $s_1$  as a function of  $f$  for different values of  $T$ . We can see that, for  $\langle k \rangle = 4$  (Fig. 11(a)),  $s_1$  approaches zero continuously as  $f$  decreases for different values of  $T$ , indicating a continuous phase transition.

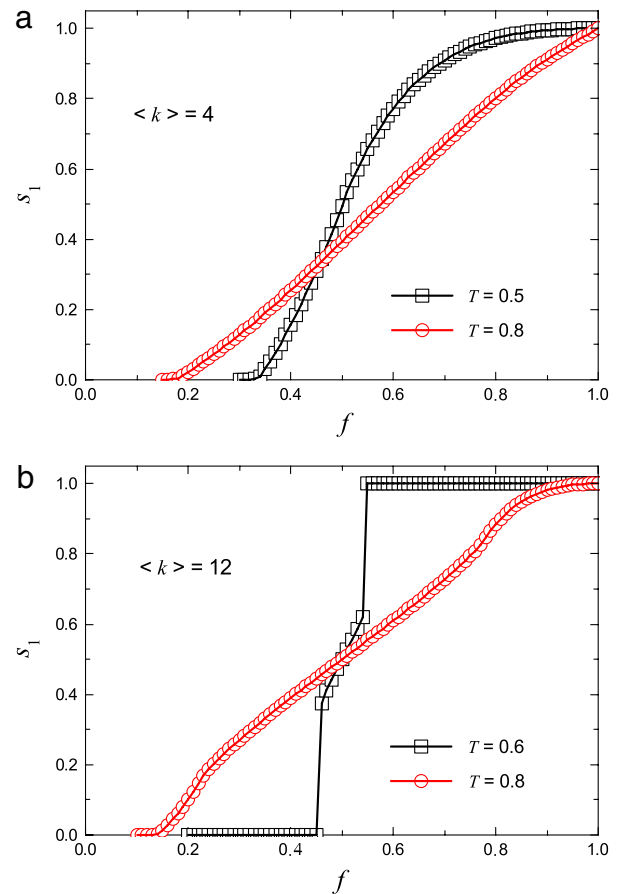


**Fig. 11.** The normalized size of the largest cluster  $s_1$  as a function of  $f$  for different values of  $T$ . The average degree of BA networks is (a)  $\langle k \rangle = 4$  and (b)  $\langle k \rangle = 12$ , respectively. The network size  $N = 5 \times 10^5$ .

While for  $\langle k \rangle = 12$  (Fig. 11(b)), there exists two abrupt transition points when  $T$  is small (e.g.,  $T = 0.6$ ), and the transition becomes continuous for a larger  $T$  ( $T = 0.8$ ). At the first abrupt transition point denoted by  $f_c$ ,  $s_1$  jumps from zero to a finite value. At the second abrupt transition point denoted by  $f_c^*$ ,  $s_1$  jumps from a finite value to one. We have checked that  $f_c + f_c^* = 1$ , which is the same as that in ER networks.

Fig. 12 shows the percolation threshold  $f_c$  as a function of  $T$  for different values of  $\langle k \rangle$ . One can see that  $f_c$  decreases as the increase

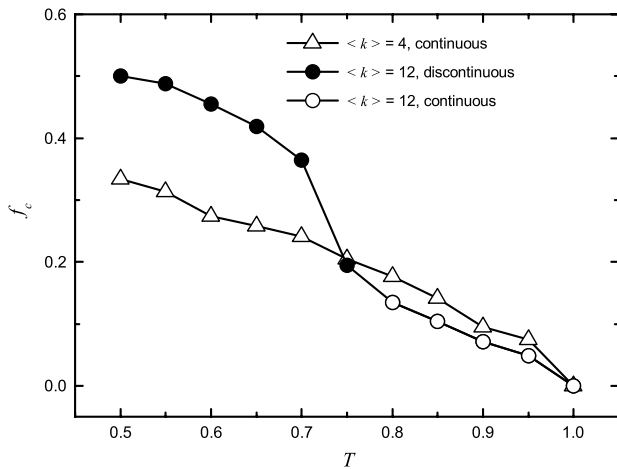


**Fig. 12.** The percolation threshold  $f_c$  as a function of  $T$  for different values of the average degree  $\langle k \rangle$  of BA networks. Filled circles denote that the phase transition is discontinuous, while empty circles and empty triangles represent that the transition is continuous.

of  $T$ . When the average degree  $\langle k \rangle$  is small (e.g.,  $\langle k \rangle = 4$ ), the percolation belongs to a continuous phase transition for all the values of  $T$ . When  $\langle k \rangle$  is large (e.g.,  $\langle k \rangle = 12$ ), the percolation behaves a discontinuous transition for the small values of  $T$  while it displays a continuous phase transition when  $T$  is large.

#### 4. Conclusions and discussions

In conclusion, we have proposed a generalized nonconsensus opinion model in which an agent changes its opinion when the fraction of nodes holding the opposite opinion in its neighborhood exceeds a threshold  $T$  ( $T \geq 0.5$ ). We apply the model on various network structures to study the formation of opinion clusters. It is found that the behavior of the normalized size of the largest cluster versus the initial concentration of nodes holding the same opinion can display a discontinuous or continuous phase transition. For regular lattices, the phase transition is continuous independent of  $T$ . For complex networks such as random networks and scale-free networks, if the average degree is small, then the phase transition is continuous, regardless of the value of  $T$ . For complex networks with the large average degree, the phase transition is continuous when  $T$  is large but it becomes discontinuous when  $T$  is small. Particularly, there exists two symmetric critical values in the case of the discontinuous phase transition. The studied opinion disappears below the first critical value while it takes over the whole population above the second critical value.

We also study the relationship between  $T$  and the percolation threshold  $f_c$  above which a large spanning cluster of nodes holding the same opinion appears. Note that when  $T = 1$ , the phase transition of our model reverts to the regular site percolation and the opinion percolation threshold is equal to that of site percolation. For square lattices, the percolation threshold  $f_c$  increases as  $T$  increases from 0.5 to 1. For Erdős–Rényi random networks with the small values of the average degree, there exists an optimal value of  $T$ , leading to the minimum  $f_c$ . For Erdős–Rényi random networks

with the large values of the average degree or Barabási–Albert scale-free networks,  $f_c$  decreases as the increase of  $T$ .

#### Acknowledgments

We thank Prof. Hai-Jun Zhou and Prof. Wen-Xu Wang for constructive comments on the manuscript. This work was supported by the National Natural Science Foundation of China under grant numbers 61403083, 11422541, 11135001 and 11375074, and the Natural Science Foundation of Fujian Province of China (Grant No. 2013J05007).

#### References

- [1] C. Castellano, S. Fortunato, V. Loreto, *Rev. Modern Phys.* 81 (2009) 591.
- [2] D.P. Landau, K. Binder, *A Guide to Monte Carlo Simulations in Statistical Physics*, third ed., Cambridge University Press, UK, 2009.
- [3] D.P. Landau, F. Wang, S.H. Tsai, *Comput. Phys. Comm.* 179 (2008) 8.
- [4] J. Yin, D.P. Landau, *Phys. Rev. E* 80 (2009) 051117.
- [5] S.H. Tsai, F.G. Wang, D.P. Landau, *Internat. J. Modern Phys. C* 20 (2009) 1357.
- [6] J.B. Santos-Filho, J.A. Plascak, D.P. Landau, *Physica A* 389 (2010) 2934.
- [7] S.H. Tsai, D.P. Landau, *Comput. Phys. Comm.* 180 (2009) 485.
- [8] C.A. Navarro, F. Canfora, N. Hitschfeld, G. Navarro, *Comput. Phys. Comm.* 187 (2015) 55.
- [9] K. Sznajd-Weron, J. Sznajd, *Internat. J. Modern Phys. C* 11 (2000) 1157.
- [10] S. Galam, *Physica A* 274 (1999) 132.
- [11] P.L. Krapivsky, S. Redner, *Phys. Rev. Lett.* 90 (2003) 238701.
- [12] S. Galam, F. Jacobs, *Physica A* 381 (2007) 366.
- [13] T.M. Liggett, *Stochastic Interacting Systems: Contact Voter, and Exclusion Processes*, Springer, Berlin, 1999.
- [14] V. Sood, S. Redner, *Phys. Rev. Lett.* 94 (2005) 178701.
- [15] A. Nowak, M. Kuś, J. Urbaniak, T. Zarycki, *Physica A* 287 (2000) 613.
- [16] M.J. de Oliveira, *J. Stat. Phys.* 66 (1992) 273.
- [17] A.D. Sánchez, J.M. López, M.A. Rodríguez, *Phys. Rev. Lett.* 88 (2002) 048701.
- [18] M. Mabilia, S. Redner, *Phys. Rev. E* 68 (2003) 046106.
- [19] S. Galam, *Physica A* 333 (2004) 453.
- [20] A. Baronchelli, L. Dall'Asta, A. Barrat, V. Loreto, *Phys. Rev. E* 76 (2007) 051102.
- [21] F. Vazquez, V.M. Eguíluz, M.S. Miguel, *Phys. Rev. Lett.* 100 (2008) 108702.
- [22] C. Castellano, M.A. Muñoz, R. Pastor-Satorras, *Phys. Rev. E* 80 (2009) 041129.
- [23] S. Mandrà, S. Fortunato, C. Castellano, *Phys. Rev. E* 80 (2009) 056105.
- [24] P. Sen, *Phys. Rev. E* 83 (2011) 016108.
- [25] Y. Wang, G. Xiao, J. Liu, *New J. Phys.* 14 (2012) 013015.
- [26] P. Chen, S. Redner, *Phys. Rev. E* 71 (2005) 036101.
- [27] L. Dall'Asta, A. Baronchelli, A. Barrat, V. Loreto, *Phys. Rev. E* 74 (2006) 036105.
- [28] C. Nardini, B. Kozma, A. Barrat, *Phys. Rev. Lett.* 100 (2008) 158701.
- [29] V. Sood, T. Antal, S. Redner, *Phys. Rev. E* 77 (2008) 041121.
- [30] C.M. Schneider-Mizell, L.M. Sander, *J. Stat. Phys.* 136 (2009) 59.
- [31] N. Masuda, N. Gibert, S. Redner, *Phys. Rev. E* 82 (2010) 010103(R).
- [32] A. Baronchelli, C. Castellano, R. Pastor-Satorras, *Phys. Rev. E* 83 (2011) 066117.
- [33] T. Takaguchi, N. Masuda, *Phys. Rev. E* 84 (2011) 036115.
- [34] A. Baronchelli, A. Díaz-Guilera, *Phys. Rev. E* 85 (2012) 016113.
- [35] C. Castellano, R. Pastor-Satorras, *Phys. Rev. E* 86 (2012) 051123.
- [36] T. Rogers, T. Gross, *Phys. Rev. E* 88 (2013) 030102(R).
- [37] V.M. Eguíluz, M.G. Zimmermann, *Phys. Rev. Lett.* 85 (2000) 5659.
- [38] B. Kozma, A. Barrat, *Phys. Rev. E* 77 (2008) 016102.
- [39] H.X. Yang, Z.X. Wu, C. Zhou, T. Zhou, B.H. Wang, *Phys. Rev. E* 80 (2009) 046108.
- [40] J. Shao, S. Havlin, H.E. Stanley, *Phys. Rev. Lett.* 103 (2009) 018701.
- [41] Q. Li, L.A. Braunstein, H. Wang, J. Shao, H.E. Stanley, S. Havlin, *J. Stat. Phys.* 151 (2013) 92.
- [42] Q. Li, L.A. Braunstein, S. Havlin, H.E. Stanley, *Phys. Rev. E* 84 (2011) 066101.
- [43] M.E.J. Newman, R.M. Ziff, *Phys. Rev. Lett.* 85 (2000) 4104.
- [44] Z. Wu, C. Lagorio, L.A. Braunstein, R. Cohen, S. Havlin, H.E. Stanley, *Phys. Rev. E* 75 (2007) 066110.
- [45] F. Radicchi, S. Fortunato, *Phys. Rev. Lett.* 103 (2009) 168701.
- [46] F. Radicchi, S. Fortunato, *Phys. Rev. E* 81 (2010) 036110.
- [47] P. Erdős, A. Rényi, *Publ. Mat.* 6 (1959) 290.
- [48] R. Parshani, S.V. Buldyrev, S. Havlin, *Proc. Natl. Acad. Sci. USA* 108 (2011) 1007.
- [49] J.H. Zhao, H.J. Zhou, Y.Y. Liu, *Nature Commun.* 4 (2013) 2412.
- [50] J. Fan, M. Liu, L. Li, X. Chen, *Phys. Rev. E* 85 (2012) 061110.
- [51] A.L. Barabasi, R. Albert, *Science* 286 (1999) 509.